BJR

Received: 29 February 2016 | Revised: 4 May 2016 | Accepted: 17 May 2016

http://dx.doi.org/10.1259/bjr.20160193

Cite this article as:
Costa F, Sarmento S, Gomes D, Magalhães H, Arrais R, Moreira G, et al. *In vivo* dosimetry using Gafchromic films during pelvic intraoperative electron radiation therapy (IOERT). *Br J Radiol* 2016; **89**: 20160193.

FULL PAPER

In vivo dosimetry using Gafchromic films during pelvic intraoperative electron radiation therapy (IOERT)

[1]FILIPA COSTA, MSc, [1,2]SANDRA SARMENTO, PhD, [3]DORA GOMES, MD, [3]HELENA MAGALHÃES, [3]ROSÁRIO ARRAIS, [4]GRACIETE MOREIRA, [4]MARIA FÁTIMA CRUZ, [5]JOSÉ PEDRO SILVA, MD, [5,6]LÚCIO SANTOS, MD, PhD and [3]OLGA SOUSA, MD

[1]Medical Physics, Radiobiology and Radiation Protection Group, IPO Porto Research Center (CI-IPOP), Portuguese Oncology Institute of Porto (IPO Porto), Porto, Portugal
[2]Medical Physics Department, Portuguese Oncology Institute of Porto (IPO Porto), Porto, Portugal
[3]Radiation Oncology Department, Portuguese Oncology Institute of Porto (IPO Porto), Porto, Portugal
[4]UCA, Portuguese Oncology Institute of Porto (IPO Porto), Porto, Portugal
[5]Surgical Oncology Department, Portuguese Oncology Institute of Porto (IPO Porto), Porto, Portugal
[6]Experimental Pathology and Therapeutics Group, IPO Porto Research Center (CI-IPOP), Portuguese Oncology Institute of Porto (IPO Porto), Porto, Portugal

Address correspondence to: Dr Sandra Sarmento
E-mail: *ssarment@gmail.com*

Objective: To characterize *in vivo* dose distributions during pelvic intraoperative electron radiation therapy (IOERT) for rectal cancer and to assess the alterations introduced by irregular irradiation surfaces in the presence of bevelled applicators.
Methods: *In vivo* measurements were performed with Gafchromic films during 32 IOERT procedures. 1 film per procedure was used for the first 20 procedures. The methodology was then optimized for the remaining 12 procedures by using a set of 3 films. Both the average dose and two-dimensional dose distributions for each film were determined. Phantom measurements were performed for comparison.
Results: For flat and concave surfaces, the doses measured *in vivo* agree with expected values. For concave surfaces with step-like irregularities, measured doses tend to be higher than expected doses. Results obtained with three films per procedure show a large variability along the irradiated surface, with important differences from expected profiles. These results are consistent with the presence of surface hotspots, such as those observed in phantoms in the presence of step-like irregularities, as well as fluid build-up.
Conclusion: Clinical dose distributions in the IOERT of rectal cancer are often different from the references used for prescription. Further studies are necessary to assess the impact of these differences on treatment outcomes. *In vivo* measurements are important, but need to be accompanied by accurate imaging of positioning and irradiated surfaces.
Advances in knowledge: These results confirm that surface irregularities occur frequently in rectal cancer IOERT and have a measurable effect on the dose distribution.

INTRODUCTION

Intraoperative electron radiation therapy (IOERT) delivers a single high dose of ionizing radiation during a surgery, for direct treatment of the tumour site and surgical bed, minimizing irradiation of the nearby sensitive tissues. A dedicated treatment-planning software was developed for IOERT; however, its use requires a CT scan of the patient.[1] This is a limitation, because pre-operative CT scans do not take into account modifications of the patient anatomy during surgery. Furthermore, intraoperative CT scans of individual patients are unfeasible in most treatments. Therefore, radiation oncologists choose IOERT applicators (diameter and bevel angle) that best suit the anatomy of the irradiated area. The electron energy will be dependent on the thickness of the irradiated area. Dose calculations are performed manually, based on dosimetric tables and dose profiles acquired in reference conditions.[2] Although this methodology is a fast and convenient way to carry out IOERT procedures, it does not allow for visualization of patient-specific dose distributions, particularly their heterogeneity.

At our institution, IOERT is used almost exclusively for locally advanced or recurrent rectal cancer, which is treated with pre-operative radiochemotherapy followed by surgery with IOERT. Rectal cancer is the second most frequent tumour treated with IOERT in Europe after breast cancer.[3] Unlike the breast, the irradiation surface for rectal cancer is usually irregular and/or concave, and 45° bevelled applicators are often used. In a previous study, Costa et al[4] have shown that an irregular irradiation surface can alter the dose distribution relative to the reference situation (flat

irradiation surface). This is particularly relevant when the entrance of a bevelled applicator is partly covered by the tissue, creating a step-like irregularity. In this situation, an adjacent hotspot is generated close to the surface, accompanied by a rapid decrease of dose at the underlying depth. The dose distribution can also be altered as a result of fluid accumulation during irradiation.[5]

Accurate dose delivery in radiotherapy is crucial to ensure local tumour control and minimize complications. International guidelines recommend prescription to the 90% isodose for adequate tumour coverage, but give no indications of acceptable uncertainties.[6] Treatment outcomes have been assessed in several studies,[7,8] but cannot be correlated with patient-specific dose distributions. In this context, it is necessary to first determine how frequently step-like surfaces occur in clinical practice and how great is the effect of clinically occurring irregularities on the dose distributions.

In vivo measurements in IOERT have been reported for treatment sites such as the breast and pancreas, where non-bevelled or small-angle applicators are commonly used and dosemeters can usually be placed on relatively flat, visually accessible surfaces. MOSFETS (metal-oxide-semiconductor field-effect transistor) detectors have been used for *in vivo* measurements, with the advantage of allowing real-time results, but they suffer from directional dependence.[5,9] Good results have also been reported by authors using films for *in vivo* dosimetry during breast IOERT.[10–12] These studies were performed with mobile LINACs specific for IOERT, such as Novac7, Liac and Mobetron. A detailed study with MOSFETS was reported for IOERT of recurrent prostate cancer, where applicators with 4–5-cm diameter and 22.5° bevel were used.[13] This specific geometry allows dose measurements directly at the point of interest, by placing the dosemeters (inserted into sterile catheters) inside the rectum or close to the bladder–urethral anastomosis. Soriani et al[13] used a Foley catheter balloon filled with a contrast medium to allow the precise identification of positioning using a C-arm mobile image intensifier. However, the same strategy cannot be applied in rectal IOERT owing to the absence of natural cavities in strategic locations.

In vivo measurements using films were introduced into our routine practice as a form of quality assurance of IOERT treatments. This work reported the first results of these *in vivo* measurements, obtained over a time period of 18 months. To our knowledge, this is the first detailed analysis of clinical dose distributions in pelvic IOERT for rectal cancer. Throughout this work, the measuring methodology was optimized to provide as much information as possible about the surface dose (D_s) distribution. Measurements in phantoms were also performed for comparison.

METHODS AND MATERIALS

LINAC system

All IOERT treatments were performed with a Varian 2100 CD (Varian Medical Systems, Palo Alto, CA) conventional LINAC adapted for IOERT with a hard-docking system of cylindrical applicators [5–10-cm diameter with bevel angles of 0° (B0), 15°, 30°(B30) and 45°(B45)]. The available energies are 6, 9, 12 and 15 MeV, with 9 MeV being the most frequently used energy. The source-to-surface distance can be varied between 124 and 144 cm (134 ± 10 cm). The LINAC bunker is located adjacent to the operating room to facilitate patient transport.

The initial characterization of the system included dosimetric measurements performed in a water phantom (MP3-M; PTW Freiburg, Freiburg im Breisgau, Germany). Percentage depth dose (PDD) curves and dose profiles were obtained using a diode (Type 60012 E; PTW-Freiburg, Freiburg im Breisgau, Germany) for all IOERT applicators, bevels and available energies. For the bevelled applicators, the PDD curves were obtained along the "clinical axis", as recommended by the American Association of Physicists in Medicine task group 48.[6] The clinical axis is defined by a line perpendicular to the phantom surface and intersecting the applicator central axis at the surface,[6] as shown in Figure 1a. For simplicity, this is referred to in the text as central axis. Absolute dose measurements were performed with both Roos (Type 34001 PTW-Freiburg, Germany) and Markus (type 23343, PTW-Freiburg, Germany) ionization chambers.

Film calibration and read-out

Measurements *in vivo* and with solid phantoms were performed using Gafchromic EBT3 (International Speciality Products, Wayne, NJ) films, which are suitable for dosimetry of high-energy electron beams.[14,15] EBT3 (the third generation of EBT films) can be handled in room light and is nearly water equivalent (effective atomic number of EBT3 is $Z_{eff\ EBT3} = 6.73$ compared with that of water $Z_{eff\ water} = 7.3$).[16] The active component of the film remained unchanged during the evolution of the EBT series.[16] Like their predecessors, EBT3 films are expected to have low energy dependence and their dose response is practically insensitive to changes in the field size, depth and dose.[16–18] In addition, they can have a high spatial resolution and can provide two-dimensional (2D) dose distributions.[14]

Film pixel value was converted into net optical density (netOD) using single-channel analysis. Following Robatjazi et al,[12] the colour channel with the greatest response gradient was used: this is the red channel below 5 Gy and the green channel above 10 Gy.[12,19] In the range of 5–10 Gy, the response gradients are similar in the red and green channels.[12,19] The green channel was chosen to analyze the *in vivo* measurements, because the D_s was expected to be ≥8.7 Gy. Solid phantoms were irradiated with lower doses (D_s approximately 3 Gy); so, the analysis was performed using the red channel. Triple-channel analysis to minimize the effect of film heterogeneities was not applied in this work.[20]

In order to convert netOD to dose, a calibration curve is needed. Square pieces of film of 5 x 5 cm^2 were placed on a solid water phantom (type RW3 PTW-Freiburg, Germany), consisting of 12 horizontal slabs, each 1-cm thick. A non-bevelled 8-cm IOERT applicator (8B0) was used to irradiate the films with a 9 MeV electron beam. 2 sets of 11 films, one placed at the surface of the phantom and the other at the depth of dose maximum (d_{max}), were irradiated independently with doses from 1 to 18 Gy. One piece of the film was left unexposed for background correction. To determine the dose delivered to the films, the LINAC output was measured following the

Figure 1. Measuring conditions: (a) the setup used to obtain the surface dose distribution for a 7-cm-diameter applicator with a 45° bevel (7B45). The EBT3 film was placed on top of a solid water phantom. (b) EBT3 films wrapped in a plastic envelope for one- and three-point *in vivo* measurements. (c) The schematic representation of a 7B45 applicator position on a pre-operative CT scan. The film location is schematized and the direction from where the photograph is taken is given by the arrow. (d) Sacral phantom (SP) with three film pieces and the 7B45 applicator positioned in such a way as to leave a step-like surface inside the applicator. (e) CT image of the SP with film locations (arrows) and film positions relative to a hypothetical flat surface and to the reference point (*R*) for the expected dose on the flat surface.

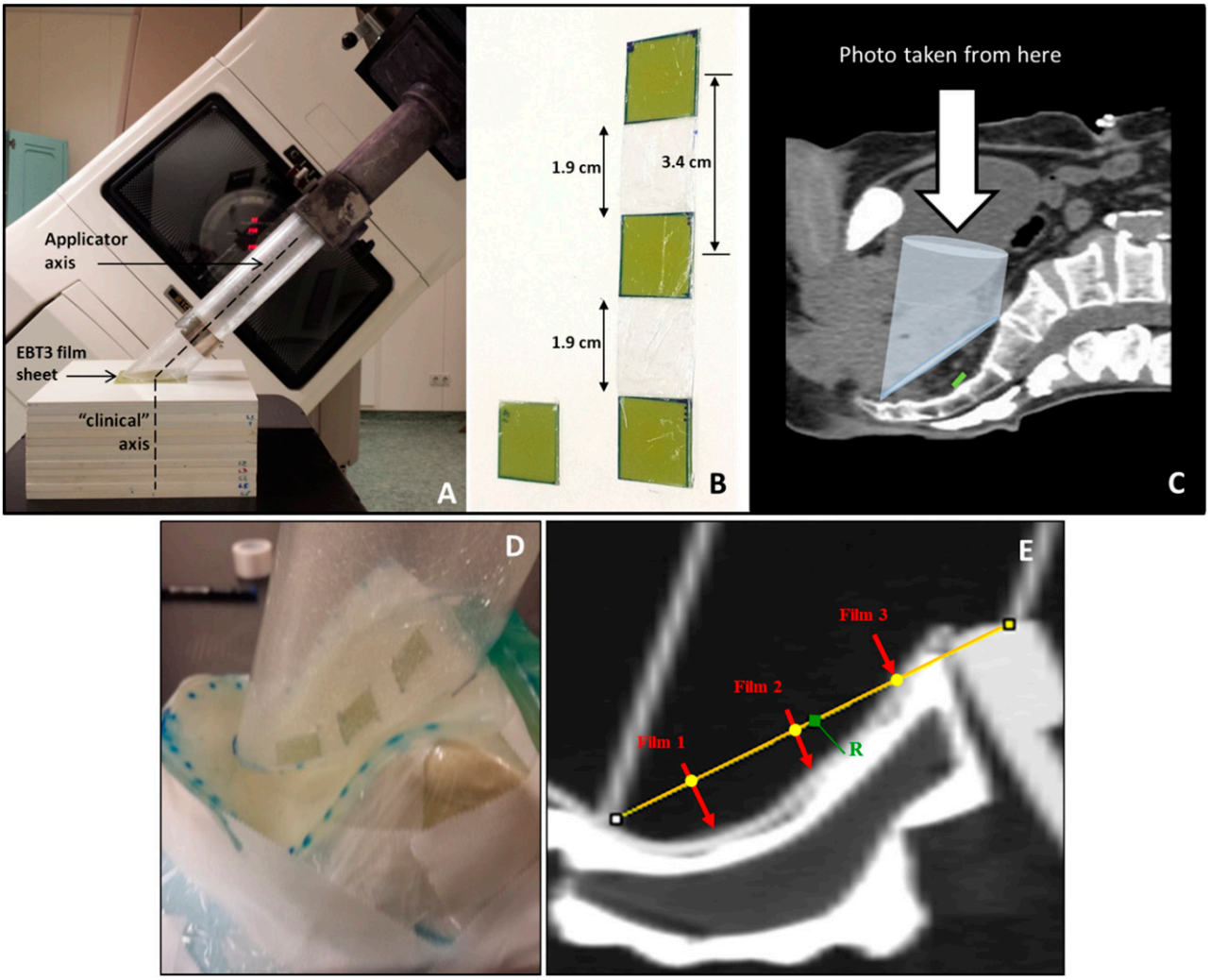

recommendations of International Atomic Energy Agency (IAEA) TRS 398[21] and by using a Markus ionization chamber placed at d_{max}.

Post-irradiation film darkening continues for at least 3 months post-exposure, particularly at higher dose levels.[22] To keep the time interval consistent between irradiation and read-out, 2 sets of 11 films were digitized 23 and 48 h after irradiation and calibration curves were obtained for both time intervals. This allowed read-out of the films used for *in vivo* measurements at the most convenient time, 23 h or 48 h after the IOERT procedure, depending on the workload and scanner occupation constraints. A region of interest (ROI) of $4.5 \times 4.5\ cm^2$ was selected for digitization to avoid border artefacts caused by cutting the film.[19] Each Gafchromic EBT3 film was placed at the centre of an Epson Expression 10000XL scanner (Seiko Epson Corp., Suwa, Japan), to avoid lateral scanner artefacts, and digitized in transmission mode and landscape orientation. The corners of the film were fixed with an adhesive tape to reduce the curling effect mentioned by the manufacturers and to minimize associated non-uniformities.[20] The images were saved as RGB and TIFF format with 72 dots per inch and analyzed using ImageJ (National Institutes of Health, Bethesda, MD) and MATLAB® (MathWorks®, Natick, MA) software. This digitization process was performed for all measurements with films in this study, either 23 or 48 h after irradiation.

A third-degree polynomial calibration curve of netOD as a function of dose was obtained for the films placed at d_{max}. This curve was used to calculate the ratio between the D_s and the dose at d_{max} (D_{max}), for the 8B0 applicator, at the central axis. Using phantom slabs of different thicknesses, the ratio D_s/D_{max} was

measured with films for every applicator, bevel and beam energy. The D_s/D_{max} ratios obtained with the films were compared with those obtained from the water tank PDD curves and the differences were found to be within 1%. PDDs in the water tank are acquired in the upwards direction to avoid surface tension effects. Since the diode has a flat top 1 mm above the point of measurement, it reaches the surface covered by water and for this reason, the D_s measured is affected by an error. The ratio D_s/D_{max} obtained with films and slab phantom seems a more reliable measurement.

Calibration was repeated every 4–5 months to account for the non-catalytic polymerization of the active molecules, or film "autodevelopment", which occurs over time even in the absence of irradiation.[23] On subsequent calibrations, irradiations were performed only with films placed at the surface, as the D_s/D_{max} ratio was already known, and the films were intended to assess surface doses. Girard et al[23] reported dose differences of up to 3.5% in the red channel for EBT2 films and calibration curves obtained 3 months apart. In this work, the difference between consecutive calibration curves obtained 4–5 months apart for EBT3 films was 3–4% for the red channel and 1.5–2% for the green channel.

Only the 8B0 applicator was used for calibration, since the applicator size has little influence on the obtained curve.[24] Energy correction to the calibration curves was not applied because the Gafchromic film energy dependence is low and the majority of the irradiations were performed with 9 MeV electron beams.[24]

Dose measurement uncertainty was calculated considering the uncertainties of the film reading and of the calibration curve fit. Uncertainties due to film reading were assessed from single film and interfilm scanner reproducibility. The total dose measurement uncertainty was found to be 2.5%. This is comparable with the total uncertainty of approximately 2% reported by Sorriaux et al[14] for 6 MeV electron beams, using two different fits according to dose range.

Measurements with solid phantoms

Surface dose distributions in reference conditions were obtained for all applicator diameters and bevel angles for a 9 MeV electron beam. Gafchromic EBT3 films were placed on top of a solid water phantom (Phantom type RW3; PTW-Freiburg, Freiburg im Breisgau, Germany), as shown in Figure 1a, and irradiated with 500 MU (D_s approximately 3 Gy). Profiles were obtained from a central rectangular ROI of 1.5-cm width, as shown in Figure 2a.The purpose of these measurements was to obtain a detailed characterization of the reference situation for comparison with *in vivo* measurements.

To obtain a realistic comparison with *in vivo* measurements, a phantom [sacral phantom (SP)] was created in house using an ORTHObones premium sacrum (3B Scientific, Valencia, Spain) with density similar to that of the human sacral bone, covered with a 3-mm thick radiotherapy bolus (Superflab; MRNI, Mount Vernon, NY), as shown in Figure 1d. Small pieces of film (1.5×1.5 cm^2) were placed on this phantom, and 3 irradiations were performed, using 9 MeV and the 7-cm diameter applicator with 45° bevel (7B45). Film locations were $R - 2.7$ cm, $R - 0.5$ cm and $R + 1.3$ cm (Figure 1e), where R is the reference point for the expected dose (D_{exp}) (centre of the applicator on a flat surface). These measurement locations were chosen to allow reproducible film positioning in phantom measurements and differ slightly from the expected film locations during *in vivo* measurements, which are $R - 3.4$ cm, R and $R + 3.4$ cm.

The effect of backscatter from the sacrum bone was evaluated separately, by placing small bone pieces on top of a solid water phantom and under the 3-mm bolus. One film piece (1.5×1.5 cm^2) was placed on top and was irradiated with 9 MeV.

In vivo measurements

In vivo measurements were performed during 32 IOERT treatments. The irradiated area included the presacral space and sometimes the lateral pelvis. The single dose was prescribed to the 90% isodose [prescribed dose (D_{pre})], and doses of 10, 12.5 and 15 Gy were chosen, depending on the assessment after tumour removal.

Two series of measurements were performed using different setups. In the first series, there was only 1 point of measurement [measured dose (D_m)] per procedure (20 patients), while in the second series (12 patients), the methodology was improved with the use of 3 points of measurement per procedure (measured doses D_{m_sup} for the upper film, D_{m_cent} for the central film and D_{m_inf} for the lower film).

Gafchromic EBT3 films were cut in small pieces of 1.5×1.5 cm^2. The small film size should not influence the film read-out, according to Moylan et al,[15] who found no significant accuracy differences between film sizes ranging from 0.5×0.5 cm^2 up to 4×4 cm^2. For the first series, the films were individually wrapped in a plastic film. For the second series, sets of three films were placed 1.9-cm apart and wrapped together, as shown in Figure 1b. Independently of the setup in use, at the operating room, the ensemble was wrapped in a sterile envelope (Tegaderm™; 3M, St. Paul, MN) and the radiation oncologist placed it on the irradiation surface, approximately at the centre of the applicator (one-point measurements), or covering the entire target surface (three-point measurements).

The attenuation of the EBT3 film wrapped in Tegaderm was determined to be <0.5%, by measuring PDD curves and absolute dose in the water tank, for 6, 9 and 12 MeV and the 7B0 applicator, without and with a disc of EBT3 (8-cm diameter, wrapped in a plastic film and Tegaderm) covering the applicator opening.

All films were marked in a corner to ensure consistent positioning and orientation in the scanner. For three-point measurements, the right corner of the top film was identified with a blue mark to allow correspondence between film positioning and the measured dose distribution. Whenever possible, the film position and irradiation surface, together with applicator position, were documented by a photograph taken before the irradiation. However, after these photographs were taken, the radiation oncologist would reposition the applicator while connecting it to the hard-docking IOERT system. The applicator position was drawn by the radiation oncologist on a planning CT image of the patient

Figure 2. Surface dose distributions obtained in phantoms: (a) dose distribution on a flat surface for an 8B45 applicator and 9 MeV (applicator positioning is shown in Figure 1a), and the region of interest (ROI) used to obtain dose profiles. (b) surface dose profiles obtained along this ROI for 6B45, 7B45 and 8B45 applicators and 9 MeV electron beam, and comparison with surface doses measured on the sacral phantom (SP) with 7B45 applicator (Figure 1d). The arrows represent probable film locations during *in vivo* measurements. (c) Two-dimensional surface dose distributions from the three films placed on the SP.

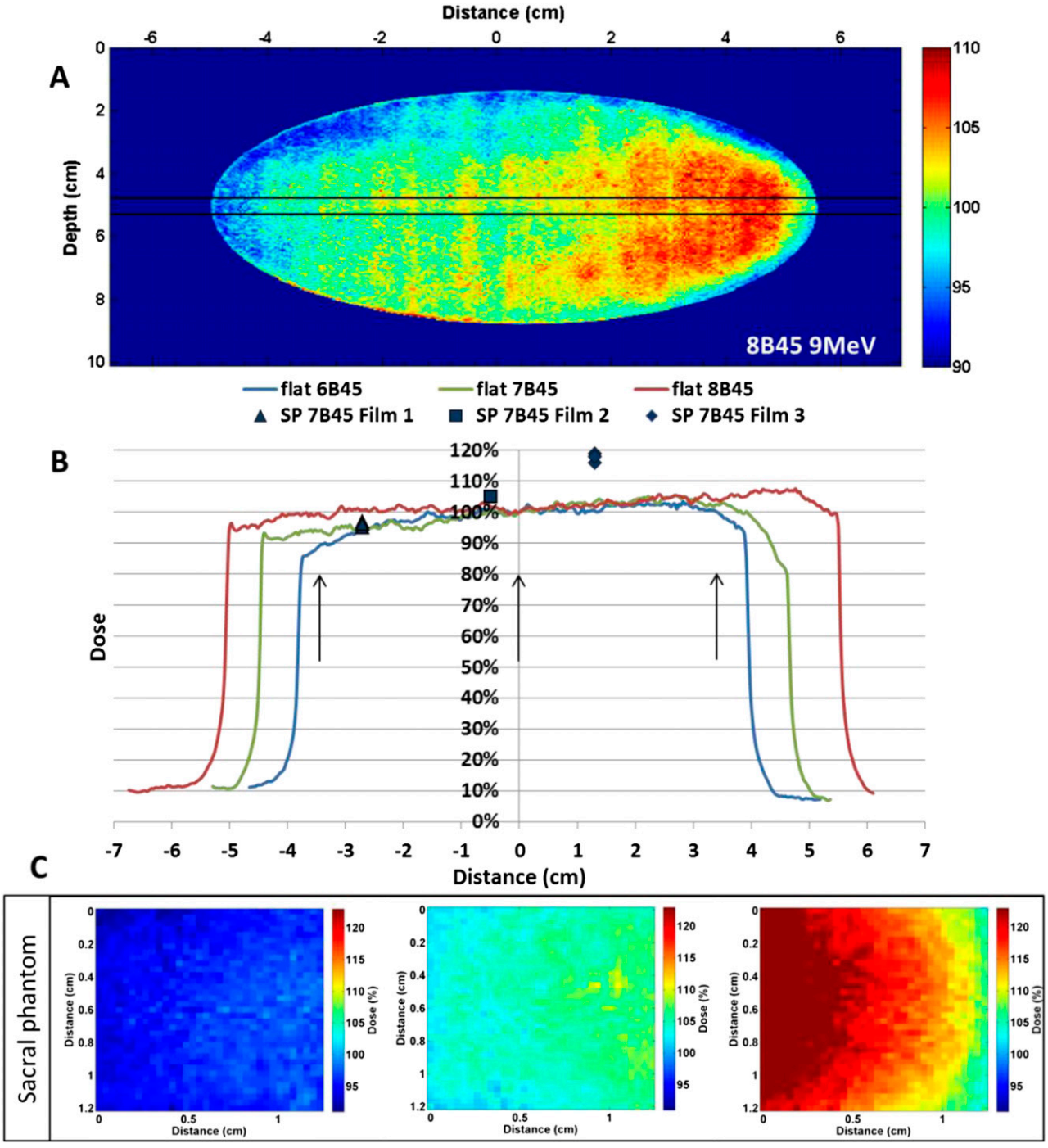

(available because all patients had been previously subjected to external beam radiotherapy). An example of this is shown in Figure 1c. Gantry angles for the performed procedures were between 0° and 30° and most frequently between 2° and 20°.

The first set of films were digitized both 23 and 48 h after irradiation, selecting an ROI of $1.2 \times 1.2\ cm^2$. After initial evaluation, this margin proved sufficient to avoid border artefacts, provided films were carefully cut with scissors, and checked visually for damage before use.[15,19] A non-irradiated film with the same dimensions was digitized for background correction. Measured doses were calculated for the 23- and 48-h digitization of each film (using the appropriate calibration curve) and were found to be consistent. Therefore, for the

Table 1. Description of the quantities presented in the study and the corresponding relationship between them

Notation in the text	Quantity description	Associated location	
		Depth	Distance from central axis (cm)
D_{max}	Maximum dose along clinical axis	d_{max}	0.0
D_s, D_{exp}	Surface dose at intersection with clinical axis in reference conditions	Surface	0.0
D_{pre}	Prescription dose	90% isodose	
D_m	Dose measured by film during one-point *in vivo* measurements	Surface	0.0 ± film displacement
D_{m_sup}	Doses measured by films during three-point *in vivo* measurements	Surface	+3.4 ± film displacement
D_{m_cent}		Surface	0.0 ± film displacement
D_{m_inf}		Surface	−3.4 ± film displacement

D_m, measured dose; d_{max}, depth of dose maximum; D_{max}, dose at d_{max}; D_{exp}, expected dose; D_{pre}, prescribed dose; D_s, surface dose.

second series of measurements, only one digitization was performed (at either 23 or 48 h, depending on time constraints).

A program was developed using MATLAB to read the mean dose obtained and display the 2D dose distributions from the digitized films, in order to analyze dose variability within the films. This proved a quick and easy way to display the data and compare them with the expected values.

When performing *in vivo* measurements with films, some authors have determined conversion factors to express measured doses at the surface as D_{max}.[11] This makes sense for nearly flat surfaces such as the breast.[4] With an irregular irradiation surface, the dose distribution relative to the reference may be significantly altered. Therefore, in this work, measured doses will be expressed directly without any conversions.

The average dose distribution measured by each film (D_m) was determined and compared with the D_{exp}, which corresponds to the central-axis D_s in reference conditions. D_{exp} was calculated based on the D_{pre} to the 90% isodose, and the ratio D_s/D_{max} determined with the films. The value of D_{max} calculated for each treatment was corrected to account for the LINAC output fluctuations using a linear correction based on periodic dose measurements performed during the time span of this study. For clarification, these quantities are summarized in Table 1.

RESULTS

Measurements in solid phantoms

The dose distribution at the surface of a solid water phantom, irradiated with a 9 MeV electron beam and an 8B45 applicator, as shown in Figure 2a. The ROI selected to obtain the dose profile along the central plane of the applicator is also displayed, as well as the resultant dose profile for B45 applicators with 6, 7 and 8 cm (Figure 2b). Clearly, the surface dose is not uniform throughout, and there are higher values closer to the shorter part (right side) of the applicator and lower values on the longest part (left side). Similar variations but with a smaller amplitude were observed for B30 applicators. For non-bevelled applicators, the surface distribution is practically homogeneous. These results are consistent with water tank profiles obtained at d_{max} and other depths for this applicator system[4] and for similar systems.[25]

During *in vivo* measurements, film placement relies on the visual estimation of the centre of the applicator. A positioning uncertainty of ±1 cm can be expected, at least for bevelled applicators and irregular surfaces. At ±1 cm from the central axis, the expected change in surface dose is ±2% (Figure 2b), which is within film measurement uncertainty. Therefore, the results of one-point measurements, and the readings of the central film in three-point measurements, should not be noticeably affected by a ±1-cm film displacement. When three films are used, the probable locations of the lateral films are ±3.4 cm away from the central axis (Figure 1b). Percentage dose values for these

Table 2. Percentage dose values expected from dose profiles obtained at the surface of a solid water phantom at ±3.4 cm from the centre (surface dose = 100% at central axis)

Applicator	Centre − 3.4 cm	Centre + 3.4 cm	Overall possible range[a] (%)
6B30	NA[b]	NA[b]	90–102
6B45	NA[b]	NA[b]	90–103
7B30	90%	99%	90–103
7B45	94%	102%	92–105
8B30	96%	103%	90–104
8B45	99%	104%	96–106

NA, not applicable.
[a]The overall possible range of dose variation reflects the maximum variation expected from the same profiles, excluding the penumbra region.
[b]The size of the 6B30 and 6B45 applicator openings is not compatible with a distance of 1.9 cm between films. Probable locations for the films inside the applicator are already considered in the overall range.

locations are shown in Table 2, together with the maximum possible range of variation (excluding the penumbra region) to account for possible film displacements.

The dose measured on the surface of a phantom with bone underneath was still in agreement with the expected reference (within experimental uncertainty), confirming that backscatter from the sacrum bone should not have a noticeable effect on *in vivo* measurements.

The surface doses measured using the SP of Figure 1d are plotted in the graph of Figure 2b, for comparison with the reference profile of the 7B45 applicator. The corresponding 2D dose distributions are shown in Figure 2c. The results obtained are different from the reference values, reaching a dose increase of 19% for the film placed at $R + 1.3$ cm. This is in good agreement with previous results obtained in phantoms, where a perfect step-like irregularity was observed to cause a lateral surface dose increase of approximately 20%.[4] The magnitude of the increase probably depends on the height of the irregularity and its location relative to the applicator, but a full characterization of possible scenarios falls outside the scope of this work. However, even a detailed phantom study cannot indicate which scenarios effectively occur in clinical practice and how often they occur. Only *in vivo* measurements can determine this.

One-point measurements (first series)

In vivo measurements were performed in 20 IOERT treatments using the first setup (first series). The results were analyzed, and the irradiation conditions are shown in Table 3, as well as the D_{pre}, the D_{exp}, which is equal to the central-axis D_s in reference conditions, and the D_m obtained from the films. The dose range measured within the 1.2×1.2 cm^2 of each film is also displayed.

As indicated in Table 3, the 9 MeV electron beam was most frequently used for the IOERT treatments, as well as the bevelled applicators, particularly the 45° bevel (80%). The 6–8-cm applicators were most frequently used, especially the 7-cm applicator.

The mean difference between D_m and D_{exp} ranged from −3.3% to +33.7%, as shown in Table 3. The D_m was higher than the expected value in 18 procedures (90%). The irradiation site can be very different from patient to patient. Based on the visual assessment and analysis of the photographs taken before the IOERT procedure, three typical irradiation surfaces were identified (Figure 3).

Table 3. Technical parameters and measurement results for the 20 intraoperative electron radiation therapy treatments where one-point measurements were performed

Procedure	*E* (MeV)	*D* (cm)	Bevel (°)	D_{pre} (Gy)	D_{exp} (Gy)	D_m (Gy)	Range (Gy)	Diff (%)	Surface
1	9	10	30	15.0	13.7	14.8	(13.8–16.1)	7.8	–
2	9	6	45	10.0	9.3	9.8	(6.1–11.7)	5.9%	–
3	9	6	45	10.0	9.3	11.1	(10.3–11.7)	19.2	–
4	12	7	45	15.0	14.2	14.5	(13.4–15.5)	2.0	–
5	9	7	45	10.0	8.9	10.4	(9.8–11.5)	16.7	–
6	9	8	45	10.0	9.3	9.6	(8.6–12.4)	3.6	–
7	9	7	0	10.0	9.4	9.2	(7.5–10.5)	−2.0	Ref
8	9	7	45	10.0	9.2	10.0	(9.4–11.0)	8.6	1
9	9	7	45	10.0	9.1	9.9	(9.4–10.5)	9.5	1
10	9	7	45	10.0	8.9	9.4	(8.8–10.0)	5.4	1
11	9	7	30	10.0	9.2	8.9	(8.2–9.3)	−3.3	1
12	9	7	45	10.0	9.1	12.2	(11.0–13.1)	33.7	2
13	9	8	45	10.0	9.2	11.0	(10.2–13.7)	19.4	2
14	9	8	45	10.0	9.2	11.2	(10.3–11.9)	21.7	2
15	9	6	45	15.0	13.6	15.1	(11.2–16.7)	10.9	2
16	9	9	30	15.0	13.3	17.1	(16.0–18.5)	28.4	2
17	9	8	45	10.0	8.9	10.5	(9.9–11.5)	17.1	2
18	9	6	45	12.5	11.3	11.5	(11.0–12.2)	1.6	2
19	9	7	45	10.0	8.9	10.8	(9.9–13.2)	21.8	2
20	9	6	45	15.0	14.0	15.4	(6.6–18.7)	9.9	2

D, applicator diameter; D_{exp}, expected dose; Diff, mean difference between measured dose and expected dose; D_m, measured dose; D_{pre}, prescribed dose; *E*, beam energy.

Figure 3. Surface types: schematic representation of typical intraoperative electron radiation therapy irradiation surface shapes, identified visually while performing *in vivo* measurements.

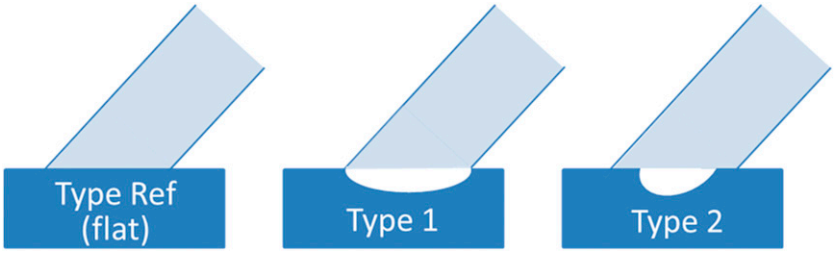

In some situations, the irradiation surface was almost flat, with soft irregularities. This type of surface is most similar to the reference conditions (type Ref.). Surface Type 1 is a relatively regular curved surface, usually created by the sacral bone curvature. The applicator can be adapted well to this type of surface. Surface Type 2 comprises situations where there is tissue partially covering the applicator or a step-like surface: this could be a partially flat or curved surface, with more or less tissue obstructing the applicator entrance and with curvatures of different depths. The phantom model shown in Figure 1d attempts to recreate an ideal Type 2 surface.

The data in Table 3 were sorted according to the type of surface identified. No identification was made for procedures where photographs could not be taken. Inside each surface type group, the data were organized by procedure date.

The 2D dose distributions within each film were analyzed in terms of uniformity and the presence of hotspots. In most cases, the dose range observed is $<\pm 2$ Gy. Higher values occurred owing to hotspots found within the films (Procedures 19 and 20) and high variability along the film (Procedures 7 and 14, which are similar to Procedure 16 but with a higher variability).

Figure 4. Three examples of one-point measurement results: Procedure 9: Type 1 surface; Procedure 17: Type 2 surface; and Procedure 16: fluid build-up is visible after irradiation (the upper left photograph was obtained before the irradiation and the lower right photograph after the irradiation). Film positioning relative to the applicator and the surface is shown in the photographs. The corresponding two-dimensional dose distributions (obtained from the films) are presented, but their orientation may differ from film orientation in the photographs (this information was not registered for these procedures).

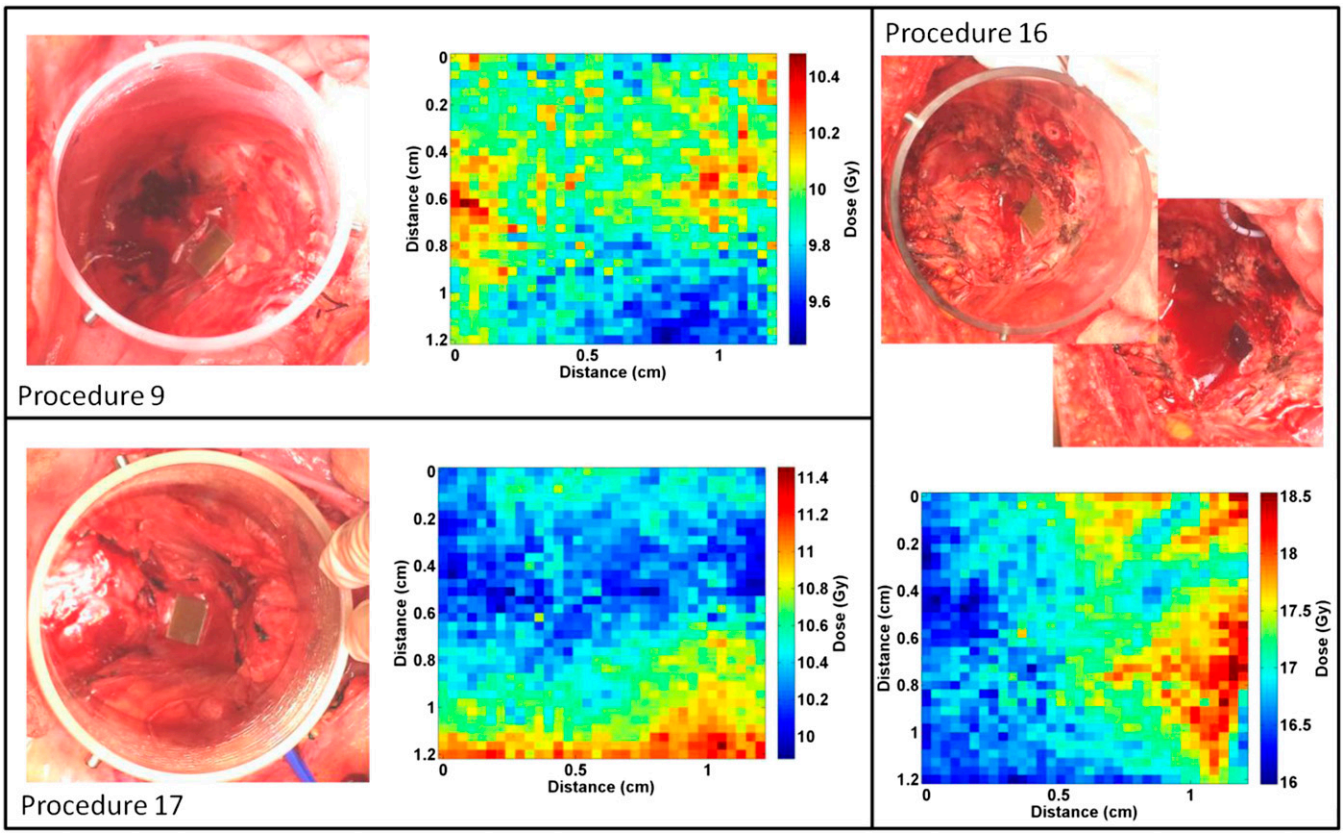

Examples of dose distributions within a film, and the corresponding photograph of the film positioning taken before irradiation, are shown in Figure 4, for a Type 1 surface (Procedure 9), Type 2 surface (Procedure 17), where the tissue covering part of the applicator entrance is visible in the photograph, and a complex situation (Procedure 16), where the film was almost completely immersed in blood at the end of the irradiation.

Three-point measurements (second series)

The results obtained for the 12 measurements performed with 3 films per procedure are shown in Table 4. To keep the methodology consistent with one-point measurements, and facilitate comparison with phantom measurements, the D_{exp} presented in Table 4 is always the D_s at the central axis in reference conditions (D_s). The D_{pre}, the D_m for each of the three films and the dose range measured within each film are also presented. D_m values are displayed according to the position of the film relative to the applicator. The first D_m results correspond to the film placed closer to the shorter part of the applicator (Figure 1c) and the others represent the central film and the one near the longest part of the applicator (placed at the bottom), respectively.

For better data assessment, the 12 procedures were divided into 3 main groups. An example of a typical irradiation surface and the respective result for each group are shown in Figure 5. The first group includes all procedures where the D_{m_cent} presents a hotspot, namely Procedures 1, 3, 6 and 12. In the example shown in Figure 5 (Procedure 3), the hotspot is also partially visible in the right-side film. Procedures where the bottom film was partially outside the applicator, or in the penumbra region, were included in the second group. An example of this is Procedure 7, as the round edge of the applicator is visible in the bottom dose distribution (left side) shown in Figure 5. The centre and right-side dose distributions resemble, respectively, the left and centre ones for Procedure 3, suggesting that the differences observed are due to displacement. Group 2 also includes Procedures 2, 10, 5 (bottom film in the penumbra region) and 9, where the bottom film was outside the applicator and the central film in the penumbra region. The third group of measurements (miscellaneous) includes one type Ref. surface (Procedure 4) and two situations which are difficult to classify (Procedures 8 and 11), because a dose reduction occurs in the middle film. As shown in Figure 5, the right-side film was in the penumbra region in Procedure 4 (type Ref.), and the dose increase on the left side (bottom) for Procedure 8 is probably related to fluid build-up.

DISCUSSION

The technical characteristics of IOERT treatments in this work (beam energy, applicator diameter and bevel used) are similar to those collected by the International Society of Intraoperative Radiation Therapy, from different European countries between 1995 and 2011, for the IOERT of rectal cancer. In the International Society of Intraoperative Radiation Therapy database, the 6-cm applicator was most frequently used (33%), followed by the 5-cm applicator (28%) and 7-cm applicator (26%), and the 45° bevel applicator was used in 83% of pelvic IOERT procedures.[3]

Analysis of the data summarized in Table 3 (for one-point measurements) suggests that lower differences between D_{exp} and D_m tend to occur when the irradiation surface is nearly flat or curved (Type 1), while higher differences are more frequently found when the tissue is covering the applicator or small holes/step-like surfaces exist (Type 2). The mean difference between D_m and D_{exp}, calculated for all one-point measurements, was 11.9%, ranging from −3.3 to 33.7%. The mean difference for Type 2 surfaces was 18.3%, ranging from 1.6 to 33.7%. For these surfaces, a difference higher than approximately10% was always observed except for Procedure 18, where the surface was so irregular that the film could not adhere to it. For Type 1 surfaces, the results were improved, with a mean difference of 5% ranging from −3.3 to 9.5%. The identified type Ref. surface showed very good agreement (−2%).

Other authors reported good agreement (within ±10%) between expected and measured doses for *in vivo* measurements performed with films during breast[10–12] and prostate[13] IOERT. However, in breast IOERT, the irradiation surface is usually flat, the radiation oncologist can visually assess the position of the film and non-bevelled applicators are most frequently used. Even in prostate IOERT, the bevel angle was only 22.5°, and it was possible to ensure a relatively flat irradiation surface.[13]

The results obtained with three-point measurements (Table 4) show great variability within each film, and between films irradiated during the same procedure. Compared with the expected central D_{exp}, the upper films (D_{m_sup}) showed a mean difference of 12.6%, the central films (D_{m_cent}) 9.3% and the bottom films (D_{m_inf}) −13.8%. The only identified flat surface (Procedure 4) showed good agreement between D_{m_cent} and D_{exp}, as well as good uniformity, considering that the right-side film was probably in the penumbra region (Figure 5).

The accurate mean value obtained for D_{m_inf} is not realistic, because some films were outside the applicator. Film displacement seems to occur more often with the three-point methodology, probably because the lateral films are close to the borders of the applicator and may be pulled during repositioning. This is a limitation of the method which still needs improvement, possibly by devising a method to photograph the irradiation surface after connection of the applicator with the LINAC.

The dose variability between films irradiated in the same procedure seems to result from a combination of different effects. For Procedures 3 (Figure 5) and 6, D_{m_inf} is approximately 6 and 10% lower than D_{m_sup}, respectively, which is in good agreement with the dose profiles expected for 8B30 and 7B45 applicators. The middle film shows a dose increase which does not appear in reference conditions, but which agrees well with the results obtained with the SP, where a dose increase of approximately 19% was observed at $R + 1.3$ cm (Figure 2). It seems reasonable to conclude that the surface shape is affecting the measured surface doses. The effect is registered more frequently by the middle film, suggesting that either the geometry is slightly different during *in vivo*

Table 4. Technical parameters and measurement results for the 12 intraoperative electron radiation therapy treatments where three-point measurements were performed. The surface type is 1 for Procedures 2, 6, 8, 9 and 10, nearly flat for Procedure 4 and Type 2 for the other procedures.

Procedure	E (MeV)	D (cm)	Bevel (°)	D_{pre} (Gy)	D_{exp} (Gy)	D_m (Gy)	Range (Gy)	Diff (%)
1	9	8	45	10	8.9	9.5	(9.2–9.9)	6.8
						11.0	(10.2–12.1)	23.5
						10.0	(9.4–11.0)	12.4
2	9	7	45	10	8.8	10.2	(9.6–10.7)	15.4
						9.4	(8.2–10.0)	5.8
						2.1[a]	(0.6–7.1)[a]	−75.8[a]
3	9	8	30	10	9.2	10.3	(9.2–11.3)	12.2
						11.5	(9.2–12.5)	25.2
						9.8	(9.1–10.4)	6.3
4	9	8	0	15	13.9	13.2	(12.2–13.5)	−6.0
						14.2	(13.6–14.4)	1.2
						14.8	(14.1–15.5)	5.5
5	9	8	30	10	9.2	11.0	(10.3–12.0)	18.8
						10.7	(10.1–11.3)	15.7
						8.7[a]	(6.7–9.7)[a]	−5.6[a]
6	9	7	45	10	9.1	10.7	(9.0–12.3)	17.4
						11.0	(9.9–11.6)	20.7
						9.7	(9.1–10.3)	6.8
7	9	7	45	10	9.1	10.8	(9.6–11.4)	16.8
						9.7	(9.1–10.0)	5.0
						7.2[a]	(2.0–9.1)[a]	−22.0[a]
8	9	9	45	15	13.8	16.0	(13.0–18.3)	16.3
						15.0	(13.9–17.5)	8.6
						17.3	(15.1–19.3)	25.6
9	9	6	45	15	13.9	17.8	(15.6–21.8)	27.5
						11.7[a]	(2.9–13.2)[a]	−16.1[a]
						1.2[a]	(0.8–1.8)[a]	−91.7[a]
10	9	7	45	10	9.3	10.8	(10.0–11.5)	16.9
						10.5	(10.1–10.9)	13.2
						6.1[a]	(1.5–9.2)[a]	−34.2[a]
11	9	6	45	10	9.4	10.6	(9.3–11.3)	12.1
						9.0	(7.6–12.2)	−4.1
						10.3	(9.3–11.4)	9.3
12	9	7	45	10	9.3	9.0	(7.2–10.3)	−2.8
						10.5	(9.9–11.1)	12.8
						9.0	(7.7–9.9)	−2.4

D, applicator diameter; D_{exp}, expected dose; Diff, mean difference between measured dose and expected dose; D_m, measured dose; D_{pre}, prescribed dose; E, beam energy.
[a]Results were obtained from films partially outside the applicator or in the penumbra region.

Figure 5. Four examples of three-point measurement results, organized by groups: Procedure 3: Group 1; Procedure 7: Group 2; Procedure 4: type Ref. surface—Group 3; and Procedure 8: miscellaneous—Group 3. Film position and orientation in the two-dimensional dose distributions is the same as in the photographs. For bevelled applicators, the longest part of the applicator appears on the left side of the photographs, which corresponds to an inferior (deeper) position than the ones on the right side. This is easily understood by observation of Figure 1c.

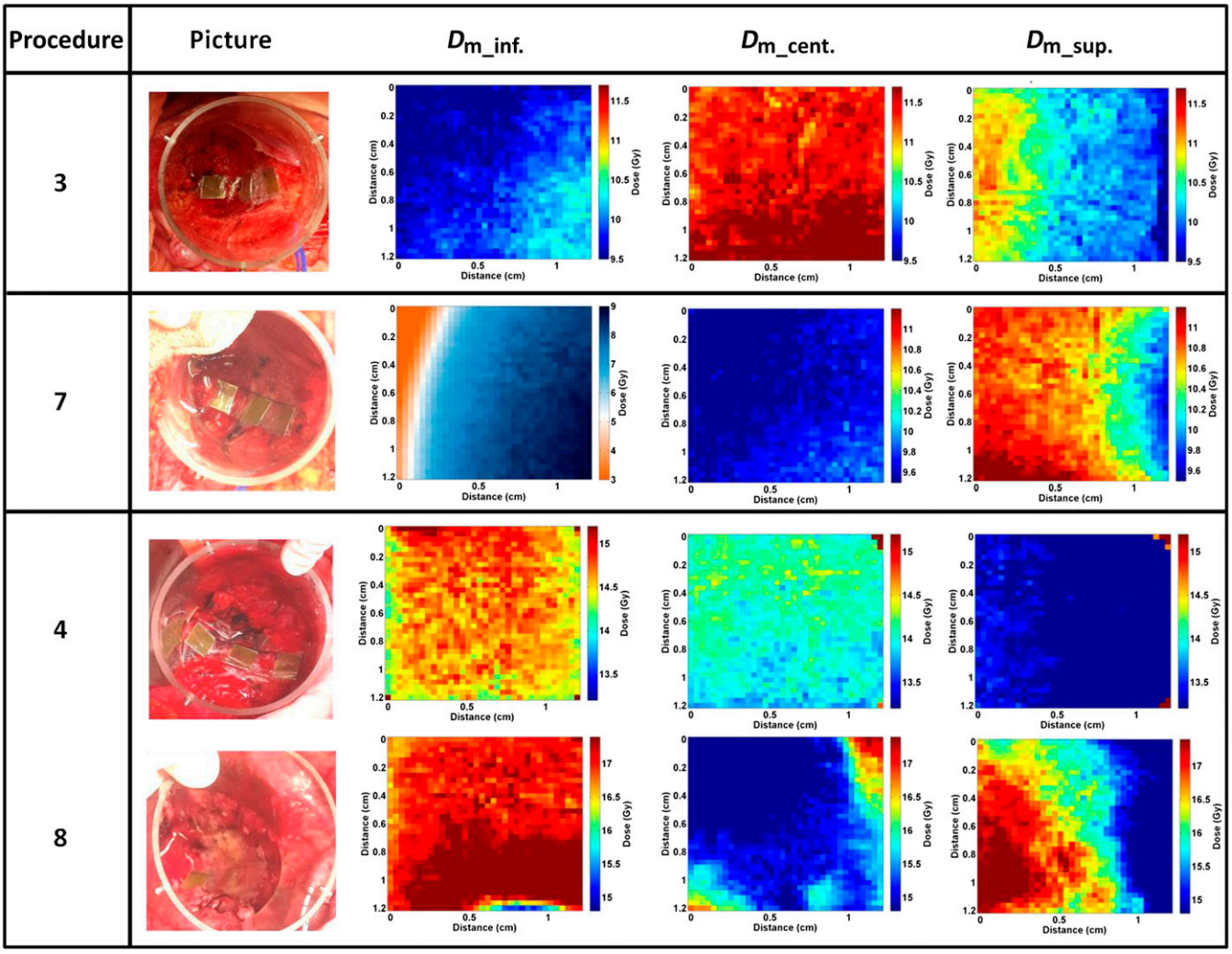

measurements or film positioning was biased towards the upper region.

The other two procedures in Group 1 (Procedures 1 and 12) also show a hotspot in the middle (increased D_{m_cent}), but the difference between D_{m_sup} and D_{m_inf} is not as expected from the reference profiles. Films located at the bottom often measured doses higher than expected, probably owing to fluid build-up. This is reflected in the values of D_{m_inf} obtained for Procedures 1, 8 and 11 (also D_{m_cent} of Procedure 10 and D_{m_sup} of Procedure 9, as the films were displaced towards the bottom).

In reference situations, the dose increase between 1- and 3-mm depth is approximately 8% for a B45 applicator, approximately 5% for B30 and approximately 4% for B0, considering an electron beam of 9 MeV. This is a significant increase over a very short distance. During this study, no information about the depth of the fluid was registered for any procedure (although there are plans to implement this in the future). The only photograph taken after irradiation [Procedure 16 of the first series—(Table 3 and Figure 4)] shows accumulation of blood in the irradiated area, but it is unknown whether this blood was actually present during irradiation, or if it accumulated outside the applicator, and flooded into the area after its removal.

Higher surface doses do not necessarily imply higher target doses. Fluid build-up shifts the whole dose distribution upwards, leading to lower doses at greater depths. Likewise, below the hotspot associated to a step-like surface, there is a rapid dose decrease in depth.[4]

The preliminary results presented in Tables 3 and 4 confirm that irregularities in the irradiation surface, especially step-like irregularities, have a measurable effect on clinical dose distributions. The sample size in this work is insufficient to determine the more

frequently occurring scenarios from statistical analysis. IOERT procedures are infrequent, making it difficult to obtain a sufficient number of measurements. More importantly, to undertake such a study, it is necessary to devise an imaging method to accurately record film and applicator position and surface shape. Nevertheless, the alteration of dose distributions caused by surface irregularities is an important finding, which can help optimize the target dose in future IOERT of rectal cancer. Radiation oncologists are advised to take into consideration the possible effects of an irregular irradiation surface, and try to minimize them whenever possible, through careful choice and positioning of IOERT applicators.

CONCLUSION

IOERT for rectal cancer is a paradigm of a difficult irradiation geometry. Our results confirm that the clinical dose distributions are different from the reference distributions used for prescription purposes, stressing the importance of *in vivo* measurements. An optimized methodology was developed, using 2D film analysis and three-point measurements, which proved an easy way to obtain important information about the surface dose distributions. Two important effects were observed: the influence of fluid build-up, which affects mostly the doses at the lowest point of measurement, and the presence of surface hotspots in the presence of step-like irregularities (*e.g.* tissue covering the entrance of the applicator). Both these effects lead to increased surface doses and a simultaneous dose reduction in depth. Further studies are necessary to assess how these alterations in clinical dose distributions may impact treatment outcomes.

ACKNOWLEDGMENTS

The authors are grateful to all other surgeons, doctors, nurses, radiotherapy technologists and physicists in the intraoperative electron radiation therapy team, for their collaboration and useful suggestions or observations, and to 3B Scientific for providing the sacral bone model.

FUNDING

This work was supported by national funds through Fundação para a Ciência e Tecnologia, in the framework of the project PTDC/SAU-ENB/117631/2010, which is co-financed by ERDF (European Regional Development Fund) through the COMPETE Programme (operational programme for competitiveness) (reference FCOMP-01-0124-FEDER-021141).

REFERENCES

1. Pascau J, Ph D, Santos A, Morillo V, Calvo FA, Bouche A, et al. An innovative tool for intraoperative electron beam radiotherapy simulation and planning: description and initial evaluation by radiation oncologists. *Int J Radiat Oncol Biol Phys* 2012; **83**: 287–95. doi: http://dx.doi.org/10.1016/j.ijrobp.2011.12.063
2. Calvo F, Meirino RM, Orecchia R. Intraoperative radiation therapy first part: rationale and techniques. *Crit Rev Oncol Hematol* 2006; **59**: 106–15. doi: http://dx.doi.org/10.1016/j.critrevonc.2005.11.004
3. Krengli M, Calvo FA, Sedlmayer F, Sole CV, Fastner G, Alessandro M, et al. Clinical and technical characteristics of intraoperative radiotherapy. Analysis of the ISIORT-Europe database. *Strahlenther Onkol* 2013; **189**: 729–37. doi: http://dx.doi.org/10.1007/s00066-013-0395-1
4. Costa F, Sarmento S, Sousa O. Assessment of clinically relevant dose distributions in pelvic IOERT using Gafchromic EBT3 films. *Phys Med* 2015; **31**: 692–701.
5. Consorti R, Petrucci A, Fortunato F, Soriani A, Marzi S, Iaccarino G, et al. *In vivo* dosimetry with MOSFETs: dosimetric characterization and first clinical results in intraoperative radiotherapy. *Int J Radiat Oncol Biol Phys* 2005; **63**: 952–60.
6. Palta JR, Biggs PJ, Hazle JD, Huq MS, Dahl RA, Ochran TG, et al. Intraoperative electron beam radiation therapy: technique,dosimetry, and dose specification: report of task force 48 of the radiation therapy committee, american association of physicists in medicine. *Int J Radiat Oncol Biol Phys* 1995; **33**: 725–46. doi: http://dx.doi.org/10.1016/0360-3016(95)00280-C
7. Dubois JB, Bussieres E, Richaud P, Rouanet P, Becouarn Y, Mathoulin-Pélissier S, et al. Intra-operative radiotherapy of rectal cancer: results of the French multi-institutional randomized study. *Radiother Oncol* 2011; **98**: 298–303.
8. Mirnezami R, Chang GJ, Das P, Chandrakumaran K, Tekkis P, Darzi A, et al. Intraoperative radiotherapy in colorectal cancer: systematic review and meta-analysis of techniques, long-term outcomes, and complications. *Surg Oncol* 2013; **22**: 22–35.
9. Tae-Suk S, Jin-Beom C, Jeong-Woo L, Doo-Hyun L, Yeon-Sil K, Bo-Young C, et al. Dosimetric characteristics of standard and micro MOSFET dosimeters as *in-vivo* dosimeter for clinical electron beam. *J Korean Phys Soc* 2009; **55**: 2566. doi: http://dx.doi.org/10.3938/jkps.55.2566
10. Severgnini M, De Denaro M, Bortul M, Vidali C, Beorchia A. *In vivo* dosimetry and shielding disk alignment verification by EBT3 GAFCHROMIC film in breast IOERT treatment. *J Appl Clin Med Phys* 2015; **16**: 112–20.
11. Ciocca M, Orecchia R, Garibaldi C, Rondi E, Luini A, Gatti G, et al. In vivo dosimetry using radiochromic films during intraoperative electron beam radiation therapy in early-stage breast cancer. *Radiother Oncol* 2003; **69**: 285–9. doi: http://dx.doi.org/10.1016/j.radonc.2003.09.001
12. Robatjazi M, Mahdavi SR, Takavr A, Baghani HR. Application of Gafchromic EBT2 film for intraoperative radiation therapy quality assurance. *Phys Med* 2015; **31**: 314–19. doi: http://dx.doi.org/10.1016/j.ejmp.2015.01.020
13. Soriani A, Landoni V, Marzi S, Iaccarino G. Setup verification and *in vivo* dosimetry during intraoperative radiation therapy for prostate cancer. *Med Phys* 2007; **34**: 3205–10.
14. Sorriaux J, Kacperek A, Rossomme S, Lee JA, Bertrand D, Vynckier S, et al. Evaluation of Gafchromic® EBT3 films characteristics in therapy photon, electron and proton beams. *Phys Med* 2013; **29**: 599–606.
15. Moylan R, Aland T, Kairn T. Dosimetric accuracy of Gafchromic EBT2 and EBT3 film for *in vivo* dosimetry. *Australas Phys Eng Sci Med* 2013; **36**: 331–7. doi: http://dx.doi.org/10.1007/s13246-013-0206-0
16. Crijns W, Maes F, van der Heide UA, van den Heuvel F. Calibrating page sized Gafchromic EBT3 films. *Med Phys* 2013; **40**: 012102. doi: http://dx.doi.org/10.1118/1.4771960
17. Devic S. Radiochromic film dosimetry: past, present, and future. *Phys Med* 2011; **27**: 122–34.
18. Devic S, Tomic N, Lewis D. Reference radiochromic film dosimetry: review of

technical aspects. *Phys Med* 2016; **32**: 541–56. doi: http://dx.doi.org/10.1016/j.ejmp.2016.02.008

19. Gafchromic® EBT2 self-developing film for radiotherapy dosimetry. Wayne, NJ: International Specialty Products; 2010.
20. van Hoof SJ, Granton PV, Landy G, Podesta M, Verhaegen F. Evaluation of a novel triple-channel radiochromic film analysis procedure using EBT2. *Phys Med Biol* 2012; **57**: 4353–68. doi: http://dx.doi.org/10.1088/0031-9155/57/13/4353
21. IAEA. *Absorbed dose determination in external beam radiotherapy: an international code of practice for dosimetry based on absorbed dose to water*, series no. 398. Vienna, Austria: International Atomic Energy Agency; 2000.
22. Palmer AL, Bradley D, Nisbet A. Evaluation and implementation of triple-channel radiochromic film dosimetry in brachytherapy. *J Appl Clin Med Phys* 2014; **15**: 280–96.
23. Girard F, Bouchard H, Lacroix F. Reference dosimetry using radiochromic film. *J Appl Clin Med Phys* 2012; **13**: 1–12.
24. Su FC, Liu Y, Stathakis S, Shi C, Esquivel C, Papanikolaou N. Dosimetry characteristics of GAFCHROMIC EBT film responding to therapeutic electron beams. *Appl Radiat Isot* 2007; **65**: 1187–92. doi: http://dx.doi.org/10.1016/j.apradiso.2007.05.005
25. Del Río J, Lázaro RA, Rojas RJ, Cores SG, Ruiz CG, Jesús M, et al. Descripción técnica y dosimétrica de un sistema aplicador de alineación rígida para radioterapia intraoperatoria con haces de electrones en acelerador convencional. *Rev Fis Med* 2013; **4**: 131–42.